Oceanologia (2018) 60, 305—311

Available online at www.sciencedirect.com

ScienceDirect

journal homepage: www.journals.elsevier.com/oceanologia/

ORIGINAL RESEARCH ARTICLE

Stokes transport in layers in the water column based on long-term wind statistics

Dag Myrhaug*, Hong Wang, Lars Erik Holmedal

Norwegian University of Science and Technology (NTNU) Trondheim, Norway

Received 6 October 2017; accepted 19 December 2017
Available online 3 February 2018

KEYWORDS
Marine litter;
Random surface gravity waves;
Stokes transport velocity;
Wind statistics

Summary This paper addresses the Stokes transport velocity for deep water random waves in given layers in the water column based on wind statistics, which can be estimated by the simple analytical tool provided here. Results are exemplified by using the Phillips and Pierson-Moskowitz model wave spectra together with long-term wind statistics from one location in the northern North Sea and from four locations in the North Atlantic. The results are relevant for e.g. assessing the drift of marine litter in the ocean based on, for example, global wind statistics.

1. Introduction

There has recently been much focus on the environmental issues related to plastic litter in the oceans; see e.g. van Sebille et al. (2015), Sherman and van Sebille (2016), Keswani et al. (2016), Brennecke et al. (2016), Avio et al. (2017); also documenting that plastic litter occurs in different layers in the water column beneath the ocean surface. One important constituent of ocean circulation models is the Stokes drift which contributes to the transport of plastic as well as microplastic located in different layers in the water column. The wave-average of the water particle trajectory in the wave propagation direction gives the Lagrangian velocity referred to as the Stokes drift, while the volume Stokes transport is obtained as the integral over the water depth of the Stokes drift (Rascle et al., 2008). The general background and further details of the Stokes drift are given in e.g. Dean and Dalrymple (1984). Myrhaug et al. (2016) gives a brief review of the literature up to that date (see the references therein). More recent works include those of Breivik et al. (2016), Li et al. (2017) and Myrhaug (2017).

The purpose of the present analytical study is to provide a simple analytical tool which yields estimates of the Stokes transport velocity for deep water random waves in given layers in the water column based on wind statistics. The Stokes transport velocity is obtained by integrating the Stokes drift between two elevations in the water column

* Corresponding author at: Department of Marine Technology, Otto Nielsens vei 10, NO-7491 Trondheim, Norway. Tel.: +47 73 59 55 27; fax: +47 73 59 55 28.
E-mail address: dag.myrhaug@ntnu.no (D. Myrhaug).
Peer review under the responsibility of Institute of Oceanology of the Polish Academy of Sciences.

Production and hosting by Elsevier

https://doi.org/10.1016/j.oceano.2017.12.004

and dividing by the distance between these two elevations. Results are exemplified by using the two model wave spectra by Phillips and Pierson-Moskowitz together with long-term wind statistics from one location in the northern North Sea and from four locations in the North Atlantic. The present results are relevant for estimating the drift of e.g. marine litter in the ocean based on global wind statistics.

2. Theoretical background

Based on classical potential wave theory the time-averaged Lagrangian drift at a z-level in the water column in a water depth d is (Dean and Dalrymple, 1984):

$$\bar{u}_L(z) = \frac{ga^2k^2}{\omega}\ \frac{\cosh 2k(z+d)}{\sinh 2kd}, \tag{1}$$

where g is the acceleration of gravity, a is the linear wave amplitude, and k is the wave number related to the cyclic wave frequency ω by the dispersion relationship

$$\omega^2 = gk \tanh kd. \tag{2}$$

According to Eq. (1) the drift of the water particles is in the direction of the wave propagation; the maximum is at the mean free surface $z = 0$, and decreases rapidly towards the sea bed as $z \to -d$ (z is positive upwards). This drift velocity is commonly referred to as Stokes drift.

When assessing the transport of material in the water column the drift velocity associated with the Stokes transport in different layers of the water column is a quantity of interest. This drift velocity is obtained by integrating Eq. (1) between two levels $z = -h_2$ and $z = -h_1$ in the water column and divided by the distance between these two levels $\Delta h = h_2 - h_1$, given as

$$v = \frac{1}{\Delta h}\int_{-h_2}^{-h_1} \bar{u}_L(z)dz = \frac{ga^2k}{2\omega} \times \frac{\sinh[2kd(1-h_1/d)]-\sinh[2kd(1-h_2/d)]}{\Delta h \cdot \sinh(2kd)}. \tag{3}$$

In deep water (i.e. for large kd and thus $\omega^2 = gk$ from Eq. (2)) the Stokes transport velocity in Eq. (3) reduces to

$$v = \frac{a^2\omega}{2\Delta h}\left(e^{-2(\omega^2/g)h_1} - e^{-2(\omega^2/g)h_2}\right). \tag{4}$$

If an individual random wave with amplitude a_n and cyclic wave frequency ω_n is considered, then the Stokes transport velocity for individual random waves in deep water is given as

$$v_n = \frac{1}{2}a_n^2\omega_n \frac{1}{\Delta h}\left(e^{-2(\omega_n^2/g)h_1} - e^{-2(\omega_n^2/g)h_2}\right). \tag{5}$$

The wave amplitude is obtained from the wave spectrum $S(\omega)$ as $a_n^2 = 2S(\omega_n)\Delta\omega$ where $\Delta\omega$ is a constant separation between frequencies. By substituting this in Eq. (5) and considering an infinite number of wave components, the total Stokes transport velocity within a sea state of random waves is obtained as

$$V = \frac{1}{\Delta h}\int_0^\infty \omega S(\omega)\,(e^{-2(\omega^2/g)h_1} - e^{-2(\omega^2/g)h_2})d\omega. \tag{6}$$

The two terms in the parenthesis of Eq. (6) represent the attenuation of the wave motion in the water column, which here is approximated by taking ω as the spectral peak frequency ω_p. As a result Eq. (6) becomes

$$V = \frac{1}{\Delta h}\left(e^{-2(\omega_p^2/g)h_1} - e^{-2(\omega_p^2/g)h_2}\right)m_1, \tag{7}$$

where m_1 is the first spectral moment obtained from the definition of the nth spectral moment

$$m_n = \int_0^\infty \omega^n S(\omega)\,d\omega; \quad n = 0, 1, 2, \ldots. \tag{8}$$

By combining Eq. (7) with the spectral mean period $T_1 = 2\pi\, m_0/m_1$, the significant wave height $H_s = 4\sqrt{m_0}$, and that there is a relationship between T_1 and the spectral peak period $T_p = 2\pi/\omega_p$, i.e. $T_1 = \gamma_1 T_p$, Eq. (7) is rearranged to

$$V = \frac{1}{\Delta h}\left(e^{-2(\omega_p^2/g)h_1} - e^{-2(\omega_p^2/g)h_2}\right)\frac{\pi H_s^2}{8\gamma_1 T_p}. \tag{9}$$

Thus, V is defined in terms of the sea state parameters H_s and T_p in deep water.

3. Example of results for two standard wave spectra and long-term wind statistics

Two standard deep water wave spectra are chosen; the Phillips and the Pierson-Moskowitz spectra, which both have been used frequently in contexts discussing the Stokes drift, e.g. see Li et al. (2017) and the references therein. The Phillips spectrum was also used by exemplifying results in Myrhaug et al. (2014, 2016) and in Myrhaug (2017), where the latter reference presented the surface Stokes drift and the Stokes transport using long-term wind statistics from the northern North Sea location used here, and from one location on the northwest Shelf of Australia.

3.1. Phillips and Pierson-Moskowitz spectra

The Phillips spectrum is (Tucker and Pitt, 2001)

$$S(\omega) = \alpha\frac{g^2}{\omega^5}, \quad \omega \geq \omega_p = \frac{g}{U_{10}}, \tag{10}$$

where $\alpha = 0.0081$ is the Phillips constant, and U_{10} is the mean wind speed at the 10 m elevation above the sea surface. By using the definition of the spectral moments in Eq. (8), it follows that

$$H_s = 4\sqrt{m_0} = \frac{2\sqrt{\alpha}}{g}U_{10}^2, \tag{11}$$

$$\gamma_1 = \frac{T_1}{T_p} = \frac{2\pi m_0}{T_p m_1} = \frac{3}{4}, \tag{12}$$

$$T_p = \frac{2\pi}{\omega_p} = \frac{2\pi}{g}U_{10}. \tag{13}$$

Furthermore, the wave length corresponding to the spectral peak period, $\lambda_p = 2\pi/k_p$, is obtained from $\omega_p^2 = gk_p$ as

$$\lambda_p = \frac{g}{2\pi} T_p^2 = \frac{2\pi}{g} U_{10}^2. \tag{14}$$

The results in the following are given for $h_1 = 0$ and $h_2 = \lambda_p/s$ where $s \geq 2$, i.e. the Stokes transport velocity corresponds to the mean drift velocity over a fraction of the wave length beneath the surface downwards in the water column. For $s = 2$ the result represents the mean drift velocity over the whole water column since the wave motion in deep water penetrates down to about half the wave length. Thus, by taking $h_1 = 0$, $h_2 = \lambda_p/s$ and substituting Eqs. (11)—(14) in Eq. (9), Eq. (9) is given in terms of U_{10} as

$$V_{Ph} = \frac{s\alpha}{6\pi}(1-e^{-4\pi/s})U_{10}$$
$$= 0.000430s(1-e^{-4\pi/s})U_{10}; s \geq 2. \tag{15}$$

The Pierson-Moskowitz (PM) spectrum with U_{10} as the parameter is (Tucker and Pitt, 2001)

$$S(\omega) = \alpha \frac{g^2}{\omega^5} \exp\left(-1.25 \frac{\omega_p^4}{\omega^4}\right), \tag{16}$$

where

$$\omega_p = \frac{2\pi}{T_p}; T_p = 0.785U_{10}, \tag{17}$$

$$H_s = 0.0246U_{10}^2, \tag{18}$$

$$T_1 = 0.606U_{10}, \tag{19}$$

$$\gamma_1 = \frac{T_1}{T_p} = 0.772, \tag{20}$$

$$\lambda_p = \frac{g}{2\pi} T_p^2 = 0.962U_{10}^2. \tag{21}$$

It should be noted that the PM spectrum was originally given with the mean wind speed at the 19.5 m elevation above the sea surface as the parameter, while the present formulation is based on taking $U_{10} = 0.93U_{19.5}$ (Tucker and Pitt, 2001). Then, by substituting these relationships in Eq. (9) the result is

$$V_{PM} = 0.000407s(1-e^{-4\pi/s})U_{10}; s \geq 2. \tag{22}$$

Thus it appears that V_{PM} is slightly smaller than V_{Ph}, i.e. the ratio is

$$\frac{V_{PM}}{V_{Ph}} = 0.947. \tag{23}$$

Fig. 1 shows examples of the Phillips and PM spectra for $U_{10} = 10$ m s^{-1} and Fig. 2 shows V/U_{10} versus s for s in the range 2—32 for the two spectra. For both spectra it appears that the ratio increases as s increases, i.e. the mean transport increases as the thickness of the layer decreases, giving ratios in the range 0.1 to about 0.5 percent. For $U_{10} = 10$ m s^{-1} this gives $\lambda_p = 64.0$ m (Eq. (14)) for the Phillips spectrum and $\lambda_p = 96.2$ m (Eq. (21)) for the PM spectrum. Thus, for s in the range 2—32, the Stokes transport velocity corresponds to the mean values over intervals from 32 m down to 2 m, respectively, for the Phillips spectrum, and over intervals from 48 m down to 3 m, respectively, for the PM spectrum.

Fig. 3 shows the corresponding results as those in Fig. 2 for the volume Stokes transport per crest length over different heights in the water column, i.e. $M = V\lambda_p/s$ versus s. For both spectra it appears that M decreases as s increases, i.e. the mean transport over a height in the water column beneath the surface decreases as the thickness of the layer decreases. As for the example discussed in Fig. 2, this means that for s in the range 2—32 the values

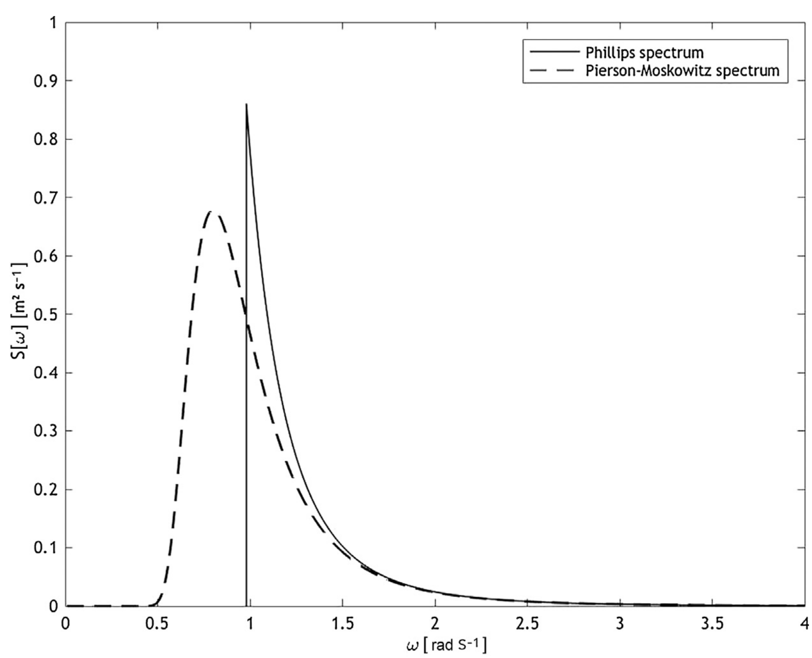

Figure 1 Phillips spectrum and Pierson-Moskowitz spectrum for $U_{10} = 10$ m s^{-1}.

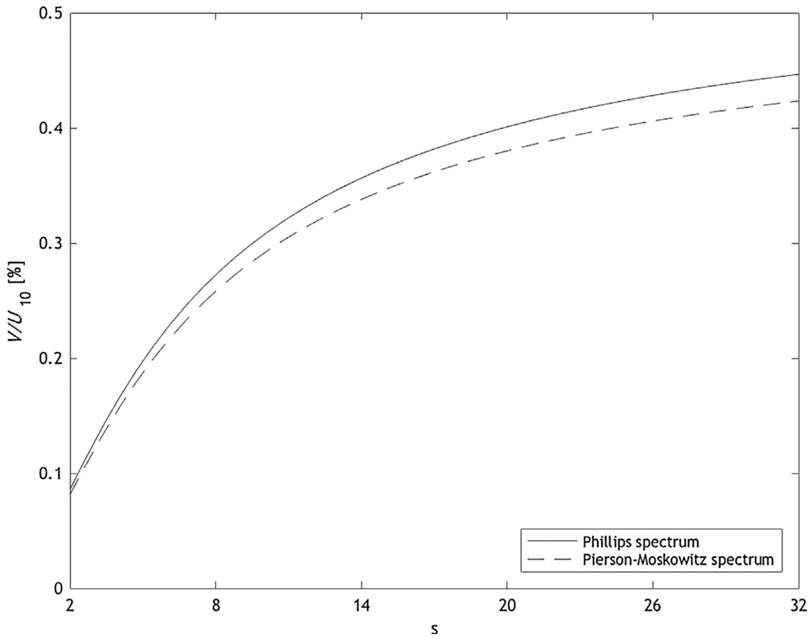

Figure 2 V/U_{10} versus s: Phillips spectrum, Eq. (15); Pierson-Moskowitz spectrum, Eq. (22).

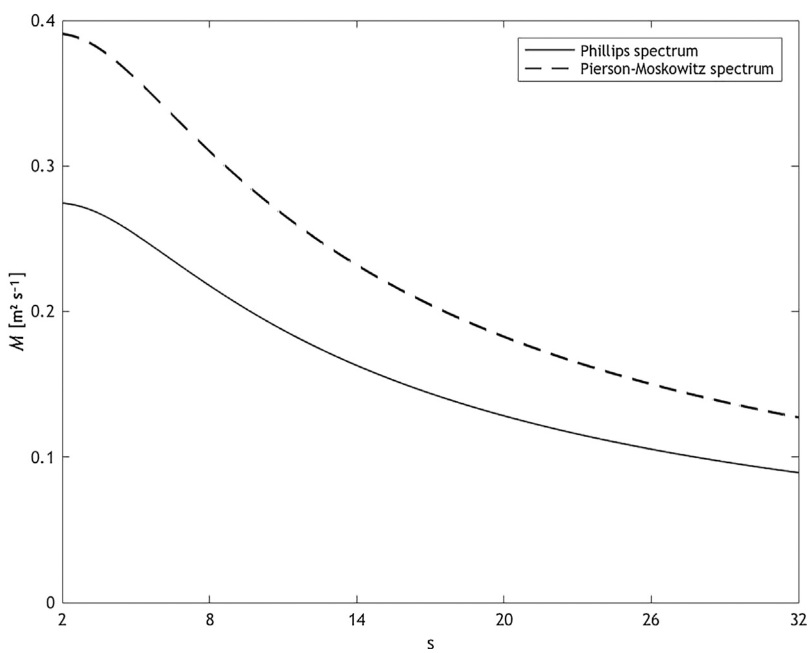

Figure 3 $M = V\lambda_p/s$ versus s corresponding to the results in Fig. 2 for the Phillips spectrum and the Pierson-Moskowitz spectrum.

of M correspond to the values over heights in the water column from 32 m below the surface to 2 m below the surface, respectively, taking the values from 0.27 $m^2\,s^{-1}$ to 0.09 $m^2\,s^{-1}$, respectively, for the Phillips spectrum. For the PM spectrum the M values are a factor 1.422 larger than those for the Phillips spectrum, taking the values 0.38—0.13 $m^2\,s^{-1}$ corresponding to the heights in the water column from 48 m below the surface to 3 m below the surface, respectively. The reason for these larger PM spectrum values is that the value of λ_p for PM is a factor 1.502 larger than that for the Phillips spectrum, i.e. due to the lower frequencies present in the PM spectrum (see Fig. 1). By considering e.g. near neutrally buoyant litter, this means that M is the volume transport (of the litter) per crest length over the given height in the water column beneath the surface due to the wave-induced drift.

3.2. Long-term wind statistics

Results for V can be obtained from available wind statistics for an ocean area, e.g. from a long-term distribution of U_{10} (see Bitner-Gregersen (2015) for a review of different parametric models for the cumulative distribution function (*cdf*) or the probability density function (*pdf*) of U_{10}). In the present examples the long-term statistics of V are exemplified by using five *cdfs* of U_{10}. First, the *cdf* of U_{10} given by Johannessen et al. (2001) is used; based on 1 hourly values of U_{10} from wind measurements covering the years (1973—1999) from the northern North Sea (NNS). Second, four *cdfs* of U_{10} given by Mao and Rychlik (2017) are used, based on estimation of Weibull *cdfs* for wind speeds along ship routes in the North Atlantic (NA) fitted to 10 years of wind speed data. The results are given for the following four locations in the North Atlantic; 20°W 60°N, 10°W 40°N, 40°W 50°N, 20°W 45°N. All these *cdfs* of U_{10} are described by the two-parameter Weibull model

$$P(U_{10}) = 1 - \exp\left[-\left(\frac{U_{10}}{\theta}\right)^{\beta}\right]; \quad U_{10} \geq 0, \tag{24}$$

with the Weilbull parameters given in Table 1.

3.3. Statistical properties of Stokes transport velocity

Now the long-term statistics of V can be derived by using the distribution of U_{10} given in Eq. (24) and Table 1. Statistical quantities of interest are e.g. the expected (mean) value of V, $E[V]$, and the variance of V, $Var[V]$, which are proportional to $E[U_{10}]$ and $Var[U_{10}]$, respectively. This requires calculation of $E[U_{10}^n]$, which for a two-parameter Weibull distributed quantity is given by (Bury, 1975)

$$E[U_{10}^n] = \theta^n \Gamma\left(1 + \frac{n}{\beta}\right), \tag{25}$$

where Γ is the gamma function. Furthermore (Bury, 1975)

$$Var[U_{10}^n] = E[U_{10}^{2n}] - (E[U_{10}^n])^2. \tag{26}$$

The results for $E[V]$ and the ratio between the standard deviation of $V (= \sqrt{Var[V]})$ and $E[V]$ (std.dev./m.v.) are given in Table 2. It should be noted that this standard deviation to mean value ratios are the same as for U_{10}. For the Phillips spectrum it appears that $E[V]$ is 0.00645 m s^{-1} (NNS) and in the range 0.00540 m s^{-1} to 0.00840 m s^{-1} (NA), where the latter value refers to the location 40°W 50°N. The values corresponding to the PM spectrum are also given, i.e. obtained by multiplying the Phillips spectrum values by a factor 0.947 (see Eq. (23)). It is also noted that the standard deviation to mean value ratios are large, i.e. in the range 43—60%.

Similarly, a characteristic value of λ_p, i.e. $E[\lambda_p]$ for the Phillips spectrum is obtained from Eq. (14) as

$$E[\lambda_p] = \frac{2\pi}{g} E[U_{10}^2], \tag{27}$$

and for the PM spectrum from Eq. (21) as

$$E[\lambda_p] = 0.962 E[U_{10}^2]. \tag{28}$$

The results are given in Table 2, showing that $E[\lambda_p]$ is in the range from about 31 m to about 73 m for the Phillips spectrum, and in the range from about 46 m to about 109 m for the PM spectrum.

A quantity of interest is the volume Stokes transport per crest length. Table 2 gives the values of $M = E[V] \cdot E[\lambda_p]/2$, i.e. the volume Stokes transport per crest length over the whole water column where there is wave activity, since the wave motion goes down to about half the wave length. For the Phillips spectrum it appears that M is 0.159 m^2 s^{-1} (NNS)

Table 1 Weibull parameters for U_{10} (see Eq. (24)) and results for $E[U_{10}]$.

North Atlantic (NA) location	θ [m s^{-1}]	β	$E[U_{10}]$ [m s^{-1}]
20°W 60°N	10.99	2.46	9.75
10°W 40°N	7.11	2.30	6.30
40°W 50°N	11.04	2.48	9.79
20°W 45°N	9.32	2.47	8.27
Northern North Sea (NNS)	8.426	1.708	7.52

Table 2 Example of results using wind statistics from the Northern North Sea (NNS) and the North Atlantic (NA), see Table 1. Results corresponding to Ph = Phillips spectrum; PM = Pierson-Moskowitz spectrum.

Distribution	$E[V]$ [m s^{-1}] Ph/PM	St.dev/m.v.	$E[\lambda_p]$ [m] Ph/PM	$M = E[V] \times E[\lambda_p]/2$ [m^2 s^{-1}] Ph/PM
NA, location				
20°W 60°N	0.00836/0.00792	0.43	72.3/108.6	0.302/0.430
10°W 40°N	0.00540/0.00511	0.46	30.8/46.3	0.083/0.118
40°W 50°N	0.00840/0.00795	0.43	72.8/109.3	0.306/0.436
20°W 45°N	0.00709/0.00671	0.43	51.9/78.0	0.184/0.262
NNS	0.00645/0.00611	0.60	49.3/74.0	0.159/0.226

and in the range 0.083 $m^2 s^{-1}$ to 0.306 $m^2 s^{-1}$ (NA), where the latter value refers to the location 40°W 50°N; for the PM spectrum the values are a factor 1.422 larger. Thus, these example calculations show that the mean value of the Stokes transport in the North Atlantic is up to a factor of about two larger than that in the northern North Sea. Furthermore, by taking the Phillips spectrum result for $M = 0.306$ $m^2 s^{-1}$ (NA) as an example, the mean volume Stokes transport $\pm$ one standard deviation is 0.18 and 0.44 $m^2 s^{-1}$, respectively, in the water column from the surface down to about 36 m. The corresponding intervals (i.e. the mean value $\pm$ one standard deviation) of the volume Stokes transport for the water columns from the surface ($z = 0$ m) to about $z = -18$ m, $z = -9$ m, $z = -4.5$ m, $z = -2.3$ m are (0.090, 0.22) $m^2 s^{-1}$, (0.045, 0.11) $m^2 s^{-1}$, (0.023, 0.055) $m^2 s^{-1}$, (0.011, 0.028) $m^2 s^{-1}$, respectively. This is of direct relevance e.g. to the volume transport of near neutrally buoyant litter as discussed in Fig. 3.

To the authors' knowledge there are limited results from observations and models to compare with. However, according to Rascle et al. (2008, Fig. 8) the surface Stokes drift U_S is about 1.3% of U_{10} in the open ocean. More specifically, in their Fig. 8 they also illustrated the variability of U_S/U_{10}, i.e. being in the range 0.4% to 1.7% for U_{10} in the range 6—10 m s^{-1}, i.e. corresponding to the range of $E[U_{10}]$ for the present data, see Table 1.

Following Webb and Fox-Kemper (2011), the unidirectional surface Stokes drift velocity within a sea state for random waves in deep water is given by

$$U_S = \frac{\pi^3 H_s^2}{g T_3^3}, \tag{29}$$

where $T_3 = 2\pi\,(m_0/m_3)^{1/3}$ is the wave period related to the surface Stokes drift velocity.

For the Phillips spectrum it follows that

$$T_3 = \frac{2^{1/3}\pi}{g} U_{10} = 0.403 U_{10}, \tag{30}$$

$$U_{SPh} = 2\alpha U_{10} = 0.0162 U_{10}. \tag{31}$$

For the PM spectrum (Tucker and Pitt, 2001)

$$m_n = \frac{1}{4}\alpha g^2 (1.25\omega_p)^{n/4-1}\Gamma\left(1-\frac{n}{4}\right). \tag{32}$$

Eq. (32) is valid for n smaller than 4, yielding $m_3 = 0.0835 U_{10}$, and thus

$$T_3 = 0.483 U_{10}, \tag{33}$$

$$U_{SPM} = 0.0170 U_{10}. \tag{34}$$

Then it follows that the ratio $E[U_S]/E[U_{10}] = U_S/U_{10}$ for both the Phillips spectrum (Eq. (31)) and the PM spectrum (Eq. (34)) is in the upper range of the results given in Rascle et al. (2008, Fig. 8) referred to, i.e. in the range 0.4—1.7%. However, e.g. by taking into account the standard deviation of the results (see Table 2), $E[U_S]$ minus one standard deviation divided by $E[U_{10}]$ will be within a wider range of these values. Although this comparison only covers the surface Stokes drift velocity it should give some confidence to the present results. However, further comparisons with observations or models for the Stokes drift in layers in the water column are also required to make firm conclusions regarding the validity of the results.

4. Conclusions

The main conclusions from this work are as follows:

1. By using the Phillips and Pierson-Moskowitz model wave spectra together with long-term wind statistics from one location in the northern North Sea and from four locations in the North Atlantic, example calculations show that the mean value of the Stokes transport in the North Atlantic is up to a factor of about two larger than that in the northern North Sea; the standard deviation to the mean value ratios are in the range 43—46% in the North Atlantic and 60% in the northern North Sea.
2. Agreement is also found between the present results and those by Rascle et al. (2008) for the surface Stokes drift velocity.

Overall, the present method can be used to assess the Stokes transport velocity for deep water random waves within sea states based on global wind statistics, which is important to estimate further the drift of e.g. near neutrally buoyant marine litter in the oceans.

Acknowledgements

This work was carried out as part of the project “Air-Sea Interaction and Transport Mechanisms in the Ocean” funded by the Norwegian Research Council (221988). This support is gratefully acknowledged.

References

Avio, C.G., Gorki, S., Regoli, F., 2017. Plastics and microplastics in the oceans: from engineering pollutants to emerged threat. Mar. Environ. Res. 128, 2—11, http://dx.doi.org/10.1016/j.marenvres.2016.05.012.

Bitner-Gregersen, E.M., 2015. Joint met-ocean description for design and operations of marine structures. Appl. Ocean Res. 51, 279—292, http://dx.doi.org/10.1016/j.apor.2015.01.007.

Breivik, Ø., Bidlot, J.-R., Janssen, A.E.M., 2016. A Stokes drift approximation based on the Phillips spectrum. Ocean Model 100, 49—56, http://dx.doi.org/10.1016/j.ocemod.2016.01.005.

Brennecke, D., Duarte, B., Paiva, F., Cacador, I., Canning-Clode, J., 2016. Microplastics as vector for heavy metal contamination from the marine environment. Estuar. Coast. Shelf Sci. 178, 189—195, http://dx.doi.org/10.1016/j.ecss.2015.12.003.

Bury, K.V., 1975. Statistical Models in Applied Science. John Wiley & Sons, New York, 646 pp.

Dean, R.G., Dalrymple, R.A., 1984. Water Wave Mechanics for Engineers and Scientists. Prentice-Hall, Inc., New Jersey, USA, 353 pp.

Johannessen, K., Meling, T.S., Haver, S., 2001. Joint distribution for wind and waves in the Northern North Sea. In: Proc. 11th Int. Offshore and Polar Engineering Conf., vol. III, Stavanger, Norway, 19—28.

Keswani, A., Oliver, D.M., Gutierrez, T., Quilliam, R.S., 2016. Microbial hitchhikers on marine plastic debris: human exposure risks at bathing water and beach environments. Mar. Environ. Res. 118, 10—19, http://dx.doi.org/10.1016/j.marenvres.2016.04.006.

Li, Q., Fox-Kemper, B., Breivik, Ø., Webb, A., 2017. Statistical models of global Langmuir mixing. Ocean Model 113, 95—114, http://dx.doi.org/10.1016/j.ocemod.2017.03.016.

Mao, W., Rychlik, I., 2017. Estimation of Weibull distribution for wind speeds along ship routes. Proc. IMechE Pt. M: J. Eng. Maritime Environ. 231 (2), 464—480, http://dx.doi.org/10.1177/1475090216653495.

Myrhaug, D., 2017. Stokes drift estimation for sea states based on long-term variation of wind statistics. Coast. Eng. J. 59 (1), 175008, http://dx.doi.org/10.1142/S0578563417500085.

Myrhaug, D., Wang, H., Holmedal, L.E., 2014. Stokes drift estimation for deep water waves based on short-term variation of wave conditions. Coastal Eng. 88, 27—32, http://dx.doi.org/10.1016/j.coastaleng.2014.01.014.

Myrhaug, D., Wang, H., Holmedal, L.E., Leira, B.J., 2016. Effects of water depth and spectral bandwidth on Stokes drift estimation based on short-term variation of wave conditions. Coastal Eng. 114, 169—176, http://dx.doi.org/10.1016/j.coastaleng.2016.04.001.

Rascle, N., Ardhuin, F., Queffeulou, P., Croizè-Fillon, D., 2008. A global wave parameter database for geophysical applications. Part 1: Wave-current-turbulence interaction parameters for the open ocean based on traditional parameterizations. Ocean Model. 25 (3—4), 154—171, http://dx.doi.org/10.1016/j.ocemod.2008.07.006.

Sherman, P., van Sebille, E., 2016. Modelling marine surface microplastic transport to assess optimal removal locations. Environ. Res. Lett. 11 (1), 014006, http://dx.doi.org/10.1088/1748-9326/11/1/014006.

Tucker, M.J., Pitt, E.G., 2001. Waves in Ocean Engineering. Elsevier, Amsterdam, 548 pp.

van Sebille, E., Wilcox, Ch., Lebreton, L., Maximenko, N., Hardesty, B.D., van Franeker, J.A., Eriksen, M., Siegel, D., Galgani, F., Law, K.L., 2015. A global inventory of small floating plastic debris. Environ. Res. Lett. 10 (12), 124006, http://dx.doi.org/10.1088/1748-9326/10/12/124006.

Webb, A., Fox-Kemper, B., 2011. Wave spectral moments and Stokes drift estimation. Ocean Model. 40, 273—288, http://dx.doi.org/10.1016/j.ocemod.2011.08.007.